This is an open access article published under a Creative Commons Attribution (CC-BY) License, which permits unrestricted use, distribution and reproduction in any medium, provided the author and source are cited.

JACS
JOURNAL OF THE AMERICAN CHEMICAL SOCIETY
Article
pubs.acs.org/JACS

Adatoms underneath Single Porphyrin Molecules on Au(111)

Johannes Mielke,[†,⊥] Felix Hanke,[‡,#] Maike V. Peters,[§] Stefan Hecht,[§] Mats Persson,[‡] and Leonhard Grill*[,†,∥]

[†]Department of Physical Chemistry, Fritz-Haber Institute of the Max-Planck Society, Faradayweg 4-6, 14195 Berlin, Germany
[‡]Surface Science Research Centre and Department of Chemistry, University of Liverpool, Liverpool L69 3BX, United Kingdom
[§]Chemistry Department, Humboldt-Universität zu Berlin, Brook-Taylor-Strasse 2, 12489 Berlin, Germany
[∥]Department of Physical Chemistry, University of Graz, Heinrichstrasse 28, 8010 Graz, Austria

Supporting Information

ABSTRACT: The adsorption of porphyrin derivatives on a Au(111) surface was studied by scanning tunneling microscopy and spectroscopy at low temperatures in combination with density functional theory calculations. Different molecular appearances were found and could be assigned to the presence of single gold adatoms bonded by a coordination bond underneath the molecular monolayer, causing a characteristic change of the electronic structure of the molecules. Moreover, this interpretation could be confirmed by manipulation experiments of individual molecules on and off a single gold atom. This study provides a detailed understanding of the role of metal adatoms in surface−molecule bonding and anchoring and of the appearance of single molecules, and it should prove relevant for the imaging of related molecule−metal systems.

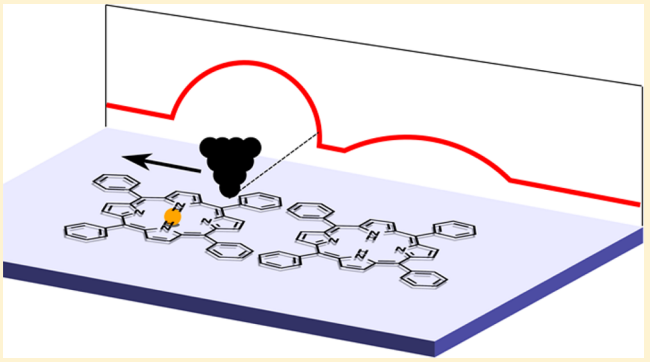

INTRODUCTION

Elementary processes between single atoms and molecules at an organic−inorganic interface are attracting a lot of attention not only for their importance in heterogeneous catalysis,[1] molecular electronics,[2] and light harvesting[3] but also from a more fundamental point of view, concerned with atom−molecule interactions. The capabilities of scanning tunneling microscopy (STM)—imaging with submolecular resolution, spectroscopy, and manipulation—can provide new insights into such elementary processes. Molecular displacement or conformational changes within a single molecule adsorbed on a metallic surface can be induced with an STM tip,[4−7] the molecular electronic structure can be investigated by spectroscopy,[8] and the catalytic role of specific inorganic structures of low coordination can be revealed.[9,10] In particular, the electronic structure of an organic molecule was found to depend strongly on the inorganic part of the interface, for instance, when reducing the coupling to the metallic surface with ultrathin NaCl films[11] or upon metalation, that is, a chemical reaction with metallic adatoms.[12]

Native adatoms are known to appear and diffuse on close-packed metal surfaces at elevated temperatures where they continuously detach from step edges.[13] Recently, they have been shown to have an important influence on the adsorption and assembly of molecules on these surfaces.[14,15] On one hand, several groups have reported trapping of copper adatoms between molecules on a Cu(110) surface,[15−17] similar to metal−ligand bonds that incorporate adatoms[18] but without forming a coordination bond. Adatoms which are diffusing along step edges of a metal surface can be trapped underneath molecules that act as templates, resulting in characteristic metallic structures of very few atoms.[19−21] On the other hand, adatoms are also involved in the bonding of sulfur-containing groups to a Au(111) surface.[22] Furthermore, thiolated molecular species form a molecule−adatom−molecule complex on Au(111) after thermal deprotonation.[23,24] In contrast to these spontaneous, thermally driven, structure formations, single adatoms can be deliberately brought in direct interaction with an individual molecule by STM manipulation.[25,26]

Here, we show from a combined scanning tunneling microscopy and density functional theory study how single adatoms on a gold surface modify the electronic structure of porphyrin molecules and thus their appearance in STM images. As a molecular system we have chosen the porphyrin derivative tetraphenylporphyrin (TPP, Figure 1a). Porphyrin derivatives are well-studied molecular compounds that are important for instance in biological processes[27] and solar energy conversion.[28] Their adsorption configuration and dynamics on surfaces have been widely studied by various techniques.[29−36] It has been found that porphyrin derivatives can adsorb in different conformations that lead to various appearances in the STM images. In particular, both planar and saddle shapes of the porphyrin macrocycle (known from molecules in solution[37])

Received: October 22, 2014
Published: December 11, 2014

 © 2014 American Chemical Society
DOI: 10.1021/ja510528x
J. Am. Chem. Soc. 2015, 137, 1844−1849

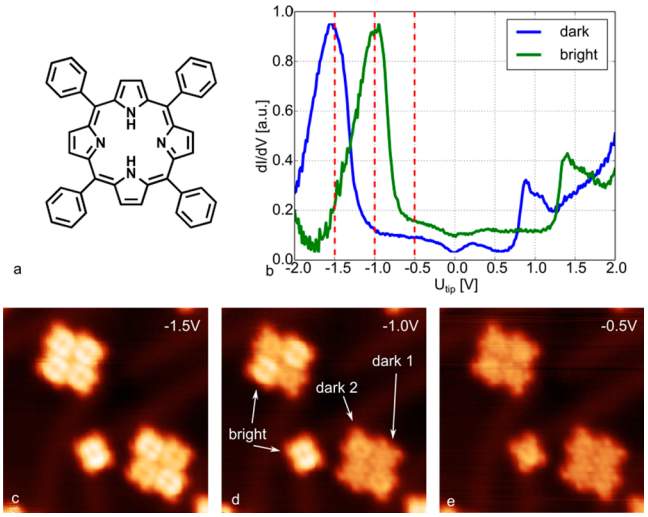

Figure 1. (a) Chemical structure of tetraphenylporphyrin (TPP). (b) dI/dV spectra of the dark and bright TPP molecules on Au(111). (c–e) STM images (11.4 × 11.4 nm^2, I_T = 0.44 nA, T = 5 K) of TPP on Au(111) with different tip bias voltages, which are indicated in the images and marked in (b) by red vertical lines.

have been found and assigned to different apparent heights in STM images.[31,32,38] In addition to the porphyrin–surface interaction that is important for the adsorption geometry, also the interaction of individual porphyrin derivatives with oxygen vacancies on a TiO_2(110) surface[38] and with individual Xe atoms on a copper surface[39] has been reported. Note that the interaction of a planar phthalocyanine molecule with its environment has recently been used to sense the bonding between atoms in the molecule with a carbon monoxide molecule at the STM tip, revealing information on the chemical structure.[40]

METHODS

Experiments were performed using a low-temperature scanning tunneling microscope (LT-STM from Omicron with Nanonis Electronics) at a temperature of about 5 K with W tips that are routinely indented into the metal surface for sharpening. All bias voltages are given for the tip with respect to the grounded sample. The Au(111) samples were cleaned by Ar^+ sputtering and subsequent annealing, and the molecules were deposited by thermal sublimation from a Knudsen cell held at 230–270 °C onto the clean Au(111) sample held at or slightly above room temperature after careful degassing of the molecules to remove possible contaminants. Density functional calculations were done using the VASP code[41] with the projector-augmented wave (PAW) method[42] and using the van der Waals density functional[43−45] with PBE exchange.[46] The adsorption of the TPP molecule on the Au surface was modeled by a single molecule adsorbed on the fcc face of the Au slab in a super cell, containing four layers of Au atoms with 56 atoms per layer, with the bottom two layers fixed. The height of the vacuum region was chosen to be at least 14 Å. The Brillouin zone was sampled using a 2×1×1 k-point grid, and the plane wave cutoff was 400 eV. STM images were simulated using the Tersoff–Hamann approximation.[47]

RESULTS AND DISCUSSION

When imaging TPP molecules, close-packed islands as well as single molecules were found on the surface (Figure 1c–e). By scanning the same area with different experimental settings, we found that the appearance of the molecules strongly depends on the applied bias voltage: At −0.5 V, all molecules appear at a similar height, while at −1 V, *dark* and *bright* molecules (henceforth, referred to as d-TPP and b-TPP, respectively) could be distinguished. At −1.5 V, the molecules were again almost identical in appearance but with a completely different appearance compared to the low bias voltage case of −0.5 V. This behavior can be understood from the dI/dV spectra of these molecules (Figure 1b). The spectra of d-TPP and b-TPP molecules have essentially the same shape but are shifted by about 0.5 eV with respect to each other. In particular, the intense dI/dV peak at −1.0 V for b-TPP, which (as discussed below in detail) derives from the lowest unoccupied molecular orbital (LUMO), is shifted down to −1.5 V for d-TPP. This peak gives rise to a large tunneling current only for the b-TPP molecule at −1.0 V and makes them brighter than the d-TPP molecules. At −1.5 V, this peak causes also a large tunneling current for the d-TPP molecules, whereas at −0.5 V there is no contribution to the tunneling current from this peak to neither b-TPP nor d-TPP, and they appear similar at these bias voltages. Hence, our experiments show that the change in STM contrast (i.e., the apparent height) is dominated by the electronic structure, and the geometric height difference does not manifest itself in the STM images (further details are presented in Supporting Information, Figure S1).

Finally, note that a periodic variation of the surface electronic structure could lead to a similar behavior, as has recently been reported for a BN/Cu(111) substrate.[48] Moreover, it has recently been found that dark and bright STM appearances of C_{60} molecules on Au(111) can be caused by diffusing substrate vacancies.[49] However, these effects can be excluded here because the spectral shift is not related to the adsorption site on the surface as we found in our calculations. Note that the molecules do not follow a periodic pattern, which has been observed for molecular appearances that are related to the adsorption site.[50] When the molecules were evaporated—deviating from the procedure described in the Methods section—onto a clean Au(111) surface held at 5 K, the molecules did not form islands, and no b-TPP could be found. Note that their abundance changes if the surface temperature varies: After heating the sample at 80 K, first b-TPP molecules appear on the elbows of the herringbone reconstruction, and if annealing is done at 130 K, b-TPP can also be found inside ordered islands (data not shown).

In previous studies, different appearances of porphyrin derivatives were assigned to different conformations[31,32,51] suggesting that the b-TPP molecules could simply be different conformations than d-TPP. However, such an assignment is not supported by our density functional theory (DFT) calculations of STM images, STS spectra, and total energies (see Supporting Information, Figures S2 and S3). The STM images and STS spectra of a d-TPP molecule are consistent with the two different saddle conformations of the adsorbed molecule shown in Figure 2a,b, which have the lowest energies and are nearly degenerate in energy. In fact, a closer inspection of a d-TPP molecule in Figure 1d shows that there are two kinds of d-TPP molecules that only differ slightly in their appearance. They are therefore identified as two tautomers of the same molecular saddle conformation (as discussed in Figure S2), but will not further be distinguished throughout this paper. Note that the planar conformation of an adsorbed TPP molecule has a substantially higher (calculated) energy than the saddle one which is probably the reason for its absence in our STM measurements. The observed rigid shift of the spectra with respect to the Fermi energy could be an indication for a charge transfer from the substrate[52] to the b-TPP molecule (similar to

DOI: 10.1021/ja510528x
J. Am. Chem. Soc. 2015, 137, 1844–1849

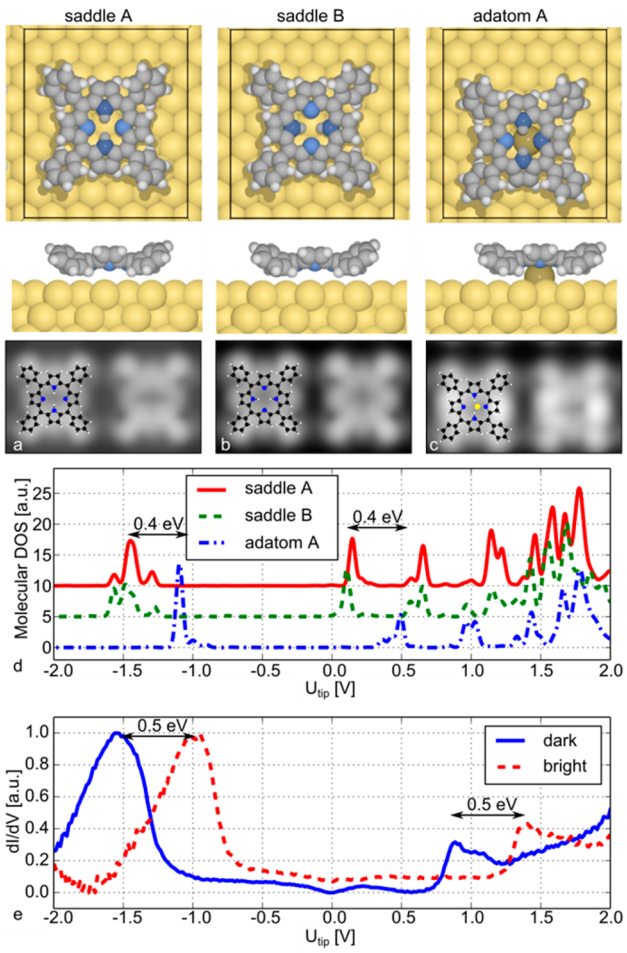

Figure 2. (a–c) Calculated adsorption geometries and simulated STM images of various configurations of TPP on Au(111). (d) Calculated local density of states and (e) dI/dV spectra from Figure 1b. The two trans tautomers of the saddle conformations in (a) and (b) correspond to the two dark states (d-TPP), and the saddle shape conformation with an Au adatom attached underneath in (c) corresponds to the bright state (b-TPP). The rigid shift of about 0.5 V of the dI/dV spectra is well reproduced in the calculations.

molecular charging on an ultrathin oxide film, resulting in a modified molecular appearance[53]), resulting in a shift of molecular orbital energies. However, since the molecules were not repelling each other, as would be expected for charged molecules,[54] the spectral shift appears to have a different origin that might be related to gold atoms on the surface.

To test this adatom hypothesis, we have done DFT calculations that compare different cases (Figure 2). The lowest energy configuration with a gold adatom corresponds to an adatom attached underneath a saddle-shaped molecular conformation (Figure 2c; other adatom positions with respect to the molecule are shown in Supporting Information, Figure S2). This configuration also yields the best agreement between the calculated STM images and density of states around the Fermi level and our experimental results for the b-TPP (see corresponding STM images in Figure 1).

On the other hand, the appearances of the two dark molecules (Figure 1d) agree well with the calculated STM images of the two states saddle A and saddle B (Figure 2a,b), and these states can therefore be assigned to two tautomers of a saddle-shaped adsorption geometry without adatom (see Figure S2 for details). Furthermore, the energy gain of the formation of the adatom A molecular state from a saddle molecular state and the adatom state is about 0.6 eV (see Supporting Information). This energy gain is due to the formation of a coordination bond between one of the N atoms in the molecule and the Au adatom with a bond distance of 2.34 Å, close to the calculated Au–N distance of 2.39 Å in Au-pyridine.[55] No such bonds are formed in the absence of the adatom since these distances are then larger than 3.7 Å.

More detailed information about the different molecular configurations on the surface is obtained from the calculated electronic density of states (DOS). The overall DOS does not change significantly for the different saddle and cis conformations of the molecule (Supporting Information, Figure S3). However, our results show very clearly that the Au adatom underneath the molecule induces a substantial energy shift of the DOS with about 0.4 eV toward positive tip voltages (i.e., toward occupied states) (Figure 2d).

This behavior is in good agreement with our experimental result (Figure 2e) where an energy shift of the entire spectrum of about 0.5 V was found. Hence, we assign the adsorbed b-TPP molecule to the attachment of a gold adatom underneath a TPP molecule having a saddle-shaped conformation. It should be noted that this phenomenon is only visible in a particular window of bias voltages (see Figure 1) and is therefore not visible in STM images taken at other bias voltages. It should be mentioned that such a phenomenon could also occur for other molecule–metal systems, and the role of adatoms should therefore be considered when interpreting STM data, since the molecular appearance and the measured electronic structure are possibly not only determined by the ideal system of a molecule on a flat surface.

The adatoms probably detach from the step edges[56] since no modification of the Au(111) herringbone reconstruction is observed, in contrast to the formation of self-assembled chemisorbed monolayers involving covalent bonding between thiolate species and individual gold atoms, which are removed from the surface and consequently lift the surface reconstruction.[23,24] Following our interpretation, we find that at low temperatures 17 ± 3% of the molecules have an adatom underneath (each molecule covers about 50 surface atoms).

Our DFT calculations also provide an understanding of the origin of the observed spectral shift between the b-TPP and d-TPP molecules. Due to the Smoluchowski effect,[57] the Au adatom is not completely screened by the conduction electrons resulting in an attractive electrostatic potential and a downward and essentially rigid shift in energy of the molecular-induced states, corresponding to an upward shift of the states in tip bias. This effect is clearly seen for the calculated projected density of states on the frontier molecular orbitals of the free molecule except for the projection on HOMO–2 for the b- and d-TPP molecules in Figure 3. Furthermore, the projection on the Au atom states show that there are no adatom-induced changes in the electronic states between −3 and +1 V tip bias ($\varepsilon_F - 1$ eV < ε < $\varepsilon_F + 3$ eV), Thus, the molecule-induced states in this energy range are not directly influenced by the presence of the adatom, and the STM contrast will be similar when sampling the states around the Fermi level. However, above +1 V tip bias (ε < $\varepsilon_F - 1$ eV), molecule-induced states, involving the lone-pair orbital of an N atom, have some overlap with adatom-induced states. This overlap is evident from the splitting of the state originating from HOMO–2 in Figure 3.

DOI: 10.1021/ja510528x
J. Am. Chem. Soc. 2015, 137, 1844–1849

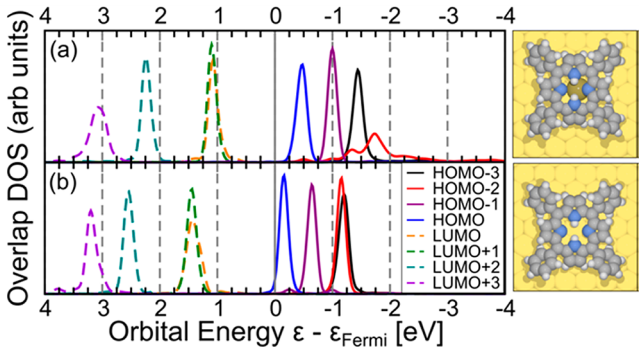

Figure 3. Calculated projected density of selected free molecule states onto the full electronic structure of (a) b-TPP and (b) d-TPP on the Au(111) surface. The energy scale was inverted in order to allow a direct comparison to the measured data (in Figure 2e).

To obtain direct experimental proof of the proposed adatom origin for the b-TPP molecule at the single-molecule level, we have artificially created single adatoms on a surface by controlled tip indentation[58] in the vicinity of a surface area of interest (see Supporting Information, Figure S4, for details). The indentation parameters were chosen carefully to avoid excessive damage of the surface (in contrast to standard tip improvement processes). From the characteristic shape of the new protrusions appearing after the tip indentation, we found that predominantly single Au atoms were created. When such a tip indentation was done in the vicinity of a molecular island, we did not only observe new gold adatoms on the metallic areas, but interestingly also an increase of the number of b-TPP molecules within the island.

This behavior is illustrated in Figure 4a,b, where one and the same molecular island was imaged before and after the creation of Au adatoms. It can clearly be seen that molecules changed from the dark to the bright state. Importantly, no reverse switching (b-TPP → d-TPP) occurred, which is in agreement with our interpretation that Au adatoms underneath the molecules are responsible for the bright state. Note that the pathway for attachment of the adatoms is unclear with two possibilites: Either adatoms diffuse on the surface over short distances, even underneath a molecular island, or the tip indentation causes stress in the surface and adatoms are pushed out directly under a molecular island, remote from the tip position.

Another confirmation of our adatom model was obtained from lateral manipulation experiments of single molecules (Figure 4c–g). At the beginning of the manipulation sequence we selected a b-TPP molecule adsorbed at an elbow of the Au(111) herringbone reconstruction (Figure 4c). After manipulating the molecule to the left, its appearance changed to d-TPP and at its former position a small protrusion was found (Figure 4d), which could be identified by its height in the STM image as an Au adatom (see Supporting Information, Figure S5). The electronic structure of the molecule in a dI/dV

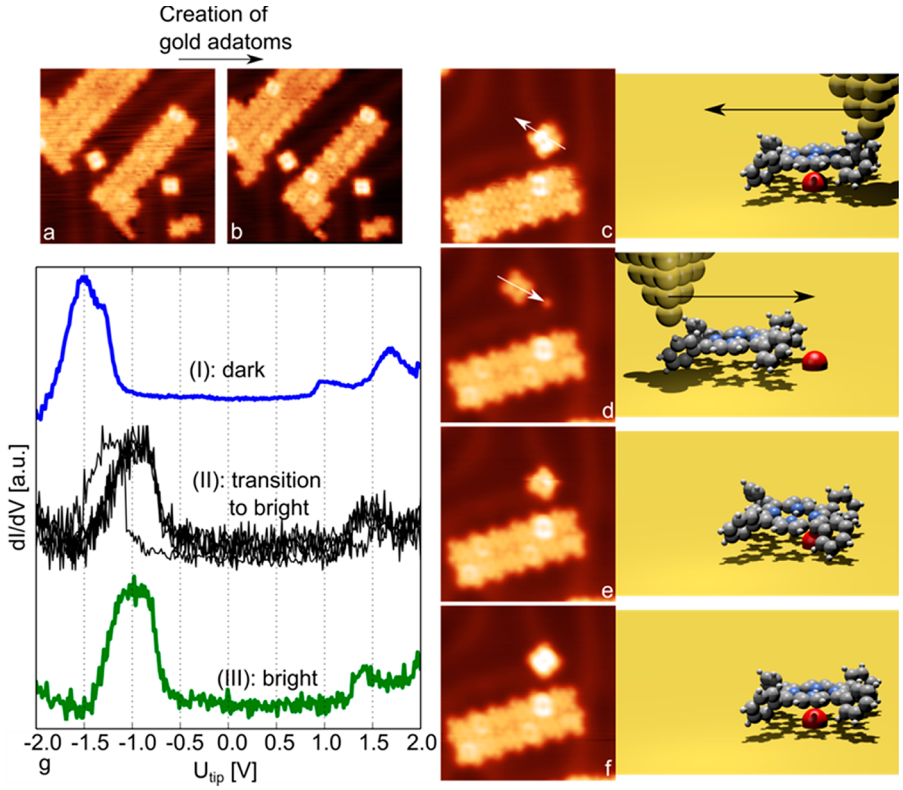

Figure 4. TPP on Au(111) before (a) and after (b) creating adatoms with a tip crash in the vicinity, changing some molecules to the bright state (17.5 × 17.5 nm^2, U_{tip} = −1 V, I = 0.18 nA, T = 5.7 K). Tip indentation is done by approaching it (from the tunneling conditions) about 3 nm toward the surface while applying +3 V to the tip. (c–f) Manipulation sequence of a bright molecule located at an elbow of the herringbone reconstruction, accompanied by sketched molecular configurations. The state of the molecule in (d–f) is confirmed by dI/dV spectroscopy (g) of the molecule. The upper and lower spectra are averaged over several sweeps. For the central one, all sweeps from +2 to −2 V are plotted, because the transition between the characteristic "dark" and "bright" spectra can be seen. Manipulation parameters: U_{tip} = 10 mV, I = 50 nA. Image parameters: 11.1 × 11.1 nm^2, U_{tip} = −1 V, I = 86 pA, T = 5.8 K.

DOI: 10.1021/ja510528x
J. Am. Chem. Soc. 2015, 137, 1844–1849

spectrum (uppermost curve in Figure 4g) confirmed that the molecule was now in the d-TPP state. Note that the dI/dV spectra in Figure 4 were not recorded with a tip optimized for spectroscopy. During such a sequence of lateral manipulation experiments, the tip apex can be easily modified, leading to slight spectral modifications (as compared to those obtained with an optimized tip in Figure 1b or Figure 2e). However, the overall spectral shape and in particular the 500 mV shift between d-TPP and b-TPP can be clearly seen. When manipulating the molecule back toward its initial position on top of the single Au adatom (as sketched in Figure 4d at the right), the molecular state in the STM image was ambiguous (Figure 4e). Hence, in order to determine its state we measured its conductance spectrum (dI/dV) by sweeping the bias voltages various times between −2 and +2 V, but this time all backward sweeps (from +2 to −2 V) are plotted (central curve in Figure 4g). In this way, the processes occurring underneath the tip could be followed in real time. During the first bias sweep from −2 to 2 V and back to −2 V, the typical features of a d-TPP molecule were recorded with the onset of the LUMO at about −1 V. Then an abrupt increase of the dI/dV curve at about −1.1 V occurred with a resulting peak at about −1.2 V, which seems to reflect an intermediate configuration between the d-TPP and b-TPP configurations in Figure 2e. In all following bias sweeps, the typical spectrum of b-TPP was recorded with the LUMO onset at about −0.7 V, which indicated that the molecule changed its state from d-TPP to b-TPP. Accordingly, the molecule was found again in the b-TPP state in the following image (Figure 4f), which was also confirmed by spectroscopy (bottom spectrum in Figure 4g). We believe that in the intermediate state (Figure 4e) the adatom is not located under the molecular center but at its periphery in an asymmetric adsorption geometry (sketched in the right panel in Figure 4e), similar to the contacting of molecular side groups with single atoms.[25] This manipulation sequence excludes hydrogen transfer between molecule and tip (as recently suggested[59]) as well as molecules in the second layer to cause the bright appearance within a molecular island.

Hence, a complete cycle from b-TPP to d-TPP and back to b-TPP can be induced in a controlled manner by lateral manipulation, thereby confirming the assignment of b-TPP to a single Au adatom underneath a molecule. This observation clearly reveals that the adatoms were not adsorbed on top of the molecules (as one might conclude from the experiments in Figure 4a,b) because in that case the molecules could not be removed from the atoms. It has been shown previously[60] that phthalocyanine molecules, which are similar to TPP molecules, behave and look differently on a surface when having their central metal atom above or below the molecular plane of the macrocycle. Consequently, as the b-TPP molecules created by crashing the tip looked identical to all other b-TPP molecules on the surface, we conclude that the adatom has always been located between the surface and the molecule.

It is important to point out that such a manipulation experiment (Figure 4c−g) was only possible when the adatom was located at an elbow site of the herringbone reconstruction, where it is more strongly bound than on other sites of the surface. We could also laterally dislocate single molecules in other surface areas, but in these cases the molecular states did not change from b-TPP to d-TPP, and no adatom was ever left behind at the former position (Supporting Information, Figure S6). This behavior indicates that the adatom was moving together with the b-TPP molecule suggesting that the adatom−TPP interaction energy exceeded the diffusion barrier of the adatom.

SUMMARY

Our combined STM-DFT study shows that native adatoms on a Au(111) surface result in a characteristic appearance of porphyrin molecules when adsorbed underneath them and the formation of a coordination bond. The characteristic contrast in this situation with a larger apparent molecular height than without an Au adatom is due to an electrostatic shift of adsorbate-induced electronic states, as observed in scanning tunneling spectroscopy experiments and corroborated by DFT calculations. The same behavior was confirmed in single-molecule manipulation experiments on and off an individual Au adatom. Although we cannot completely exclude that also rare residual contaminants on the metal surface might modify the molecular appearance, our STM manipulation, spectroscopy, and calculation results give compelling evidence that the origin of the brighter molecular appearance is the gold adatoms. Our studies illustrate the key importance of carefully considering native adatoms in the molecule−surface bonding and anchoring when interpreting STM data of molecular nanostructures on metal surfaces.

ASSOCIATED CONTENT

Supporting Information

Origin of the STM contrast; investigation of different molecular configurations by DFT; creation of gold adatoms; adatom heights; lateral manipulation of single molecules; and additional references. This material is available free of charge via the Internet at http://pubs.acs.org.

AUTHOR INFORMATION

Corresponding Author

leonhard.grill@uni-graz.at

Present Addresses

[⊥]J.M.: BAM Bundesanstalt für Materialforschung and -prüfung, Berlin, Germany

[#]F.H.: Biovia, 334 Science Park, Cambridge CB4 0WN, UK

Notes

The authors declare no competing financial interest.

ACKNOWLEDGMENTS

We are grateful to the European Union (ARTIST and AtMol projects) for financial support and EPSRC (EP/L000202) through MCC, and SNIC for computer resources at HECTOR and PDC.

REFERENCES

(1) Ertl, G.; Knözinger, H.; Schüth, F.; Weitkamp, J. *Handbook of Heterogeneous Catalysis*; Wiley-VCH: Weinheim, 2008.
(2) Heath, J. R.; Ratner, M. A. *Phys. Today* **2003**, *56*, 43−49.
(3) Imahori, H.; Norieda, H.; Yamada, H.; Nishimura, Y.; Yamazaki, I.; Sakata, Y.; Fukuzumi, S. *J. Am. Chem. Soc.* **2001**, *123*, 100−110.
(4) Stroscio, J. A.; Eigler, D. M. *Science* **1991**, *254*, 1319−1326.
(5) Moresco, F. *Phys. Rep.* **2004**, *399*, 175−225.
(6) Otero, R.; Rosei, F.; Besenbacher, F. *Annu. Rev. Phys. Chem.* **2006**, *57*, 497−525.
(7) Grill, L. *J. Phys.: Condens. Matter* **2008**, *20*, 053001.
(8) Hipps, K. W.; Barlow, D. E.; Mazur, U. *J. Phys. Chem. B* **2000**, *104*, 2444−2447.
(9) Zambelli, T.; Wintterlin, J.; Trost, J.; Ertl, G. *Science* **1996**, *273*, 1688−1690.

DOI: 10.1021/ja510528x
J. Am. Chem. Soc. 2015, 137, 1844−1849

(10) Saywell, A.; Schwarz, J.; Hecht, S.; Grill, L. *Angew. Chem., Int. Ed.* **2012**, *51*, 5096−5100.
(11) Repp, J.; Meyer, G.; Stojkovic, S.; Gourdon, A.; Joachim, C. *Phys. Rev. Lett.* **2005**, *94*, No. 026803.
(12) Kretschmann, A.; Walz, M.-M.; Flechtner, K.; Steinrück, H.-P.; Gottfried, J. M. *Chem. Commun.* **2007**, *2007*, 568−570.
(13) Giesen, M. *Prog. Surf. Sci.* **2001**, *68*, 1−153.
(14) Matena, M.; Stöhr, M.; Riehm, T.; Björk, J.; Martens, S.; Persson, M.; Llobo-Checa, J.; Mueller, K.; Wadepohl, H.; Zegenhagen, J.; Jung, T. A.; Gade, L. H. *Chem.—Eur. J.* **2010**, *16*, 2079−2091.
(15) Raval, R.; Haq, S.; Hanke, F.; Dyer, M. S.; Persson, M.; Iavicoli, P.; Amabilino, D. *J. Am. Chem. Soc.* **2011**, *133*, 12031−12039.
(16) Dong, L.; Sun, Q.; Zhang, C.; Li, Z.; Sheng, K.; Kong, H.; Tan, Q.; Pan, Y.; Hu, A.; Xu, W. *Chem. Commun.* **2013**, *49*, 1735−1737.
(17) Hanke, F.; Haq, S.; Raval, R.; Persson, M. *ACS Nano* **2011**, *5*, 9093−9103.
(18) Lin, N.; Stepanow, S.; Ruben, M.; Barth, J. V. *Top. Curr. Chem.* **2009**, *287*, 1−44.
(19) Rosei, F.; Schunack, M.; Jiang, P.; Gourdon, A.; Lagsgaard, E.; Stensgaard, I.; Joachim, C.; Besenbacher, F. *Science* **2002**, *296* (5566), 328−331.
(20) Otero, R.; Rosei, F.; Naitoh, Y.; Jiang, P.; Thostrup, P.; Gourdon, A.; Laegsgaard, E.; Stensgaard, I.; Joachim, C.; Besenbacher, F. *Nano Lett.* **2004**, *4*, 75−78.
(21) Grill, L.; Rieder, K.-H.; Moresco, F.; Stojkovic, S.; Gourdon, A.; Joachim, C. *Nano Lett.* **2005**, *5*, 859−863.
(22) Maksymovych, P.; Sorescu, D. C.; Yates, J. T. *Phys. Rev. Lett.* **2006**, *97*, No. 146103.
(23) Maksymovych, P.; Yates, J. T. *J. Am. Chem. Soc.* **2008**, *130*, 7518−7519.
(24) Voznyy, O.; Dubowski, J. J.; Yates, J. T.; Maksymovych, P. *J. Am. Chem. Soc.* **2009**, *131*, 12989−12993.
(25) Soe, W.-H.; Manzano, C.; Renaud, N.; Mendoza, P. d.; Sarkar, A. D.; Ample, F.; Hliwa, M.; Echavarren, A. M.; Chandrasekhar, N.; Joachim, C. *ACS Nano* **2011**, *5*, 1436−1440.
(26) Kumagai, T.; Hanke, F.; Gawinkowski, S.; Sharp, J.; Kotsis, K.; Waluk, J.; Persson, M.; Grill, L. *Nat. Chem.* **2014**, *6*, 41−46.
(27) Shelnutt, J. A.; Song, X.-Z.; Ma, J.-G.; Jia, S.-L.; Jentzena, W.; Medforth, C. J. *Chem. Soc. Rev.* **1998**, *27*, 31−41.
(28) Li, L.-L.; Diau, E. W.-G. *Chem. Soc. Rev.* **2012**, *42*, 291−304.
(29) Jung, T. A.; Schlittler, R. R.; Gimzewski, J. K. *Nature* **1997**, *386*, 696−698.
(30) Moresco, F.; Meyer, G.; Rieder, K.-H.; Tang, H.; Gourdon, A.; Joachim, C. *Phys. Rev. Lett.* **2001**, *86*, 672−675.
(31) Qiu, X. H.; Nazin, G. V.; Ho, W. *Phys. Rev. Lett.* **2004**, *93*, No. 196806.
(32) Iancu, V.; Deshpande, A.; Hla, S.-W. *Nano Lett.* **2006**, *6*, 820−823.
(33) Auwärter, W.; Weber-Bargioni, A.; Riemann, A.; Schiffrin, A.; Gröning, O.; Fasel, R.; Barth, J. V. *J. Chem. Phys.* **2006**, *124*, No. 194708.
(34) Müllegger, S.; Schöfberger, W.; Rashidi, M.; Reith, L. M.; Koch, R. *J. Am. Chem. Soc.* **2009**, *131*, 17740−17741.
(35) Buchner, F.; Xiao, J.; Zillner, E.; Chen, M.; Röckert, M.; Ditze, S.; Stark, M.; Steinrück, H.-P.; Gottfried, J. M.; Marbach, H. *J. Phys. Chem. C* **2011**, *115*, 24172−24177.
(36) Kumagai, T.; Hanke, F.; Gawinkowski, S.; Sharp, J.; Kotsis, K.; Waluk, J.; Persson, M.; Grill, L. *Phys. Rev. Lett.* **2013**, *111*, No. 246101.
(37) Unger, E.; Beck, M.; Lipski, R. J.; Dreybrodt, W.; Medforth, C. J.; Smith, K. M.; Schweitzer-Stenner, R. *J. Phys. Chem. B* **1999**, *103*, 10022−10031.
(38) Lackinger, M.; Janson, M. S.; Ho, W. *J. Chem. Phys.* **2012**, *137*, No. 234707.
(39) Qiu, X.; Nazin, G. V.; Hotzel, A.; Ho, W. *J. Am. Chem. Soc.* **2002**, *124*, 14804−14809.
(40) Chiang, C.-I.; Xu, C.; Han, Z.; Ho, W. *Science* **2014**, *344*, 885−888.
(41) Kresse, G.; Furthmüller, J. *Comput. Mater. Sci.* **1996**, *6*, 15−50.
(42) Kresse, G.; Joubert, D. *Phys. Rev. B* **1999**, *59*, 1758−1775.
(43) Dion, M.; Rydberg, H.; Schröder, E.; Langreth, D. C.; Lundqvist, B. I. *Phys. Rev. Lett.* **2004**, *92*, No. 246401.
(44) Klimes, J.; Bowler, D. R.; Michaelides, A. *Phys. Rev. B* **2011**, *83*, No. 195131.
(45) Thonhauser, T.; Cooper, V. R.; Li, S.; Puzder, A.; Hyldgaard, P.; Langreth, D. C. *Phys. Rev. B* **2007**, *76*, No. 125112.
(46) Perdew, J. P.; Burke, K.; Ernzerhof, M. *Phys. Rev. Lett.* **1996**, *77*, 3865−3868.
(47) Tersoff, J.; Hamann, D. R. *Phys. Rev. Lett.* **1983**, *50*, 1998−2001.
(48) Joshi, S.; Bischoff, F.; Koitz, R.; Ecija, D.; Seufert, K.; Seitsonen, A. P.; Hutter, J.; Diller, K.; Urgel, J. I.; Sachdev, H.; Barth, J. V.; Auwärter, W. *ACS Nano* **2013**, *8*, 430−442.
(49) Shin, H.; Schwarze, A.; Diehl, R. D.; Pussi, K.; Colombier, A.; Gaudry, E.; Ledieu, J.; McGuirk, G. M.; Loli, L. N. S.; Fournee, V.; Wang, L. L.; Schull, G.; Berndt, R. *Phys. Rev. B* **2014**, *89*, No. 245428.
(50) Dri, C.; Peters, M. V.; Schwarz, J.; Hecht, S.; Grill, L. *Nat. Nanotechnol.* **2008**, *3*, 649−653.
(51) Ditze, S.; Stark, M.; Buchner, F.; Aichert, A.; Jux, N.; Luckas, N.; Görling, A.; Hieringer, W.; Hornegger, J.; Steinrück, H.-P.; Marbach, H. *J. Am. Chem. Soc.* **2014**, *136*, 1609−1616.
(52) Braun, K.-F.; Hla, S. W. *J. Chem. Phys.* **2008**, *129*, No. 064707.
(53) Mikaelian, G.; Ogawa, N.; Tu, X. W.; Ho, W. *J. Chem. Phys.* **2006**, *124*, No. 131101.
(54) Wegner, D.; Yamachika, R.; Wang, Y.; Brar, V. W.; Bartlett, B. M.; Long, J. R.; Crommie, M. F. *Nano Lett.* **2008**, *8*, 131−135.
(55) Wu, D.-Y.; Ren, B.; Jiang, Y.-X.; Xu, X.; Tian, Z.-Q. *J. Phys. Chem. A* **2002**, *106*, 9042−9052.
(56) Brune, H. *Surf. Sci. Rep.* **1998**, *31*, 121−229.
(57) Smoluchowski, R. *Phys. Rev.* **1941**, *60*, 661−674.
(58) Hla, S.-W.; Braun, K.-F.; Iancu, V.; Deshpande, A. *Nano Lett.* **2004**, *4*, 1997−2001.
(59) Smykalla, L.; Shukrynau, P.; Mende, C.; Rüffer, T.; Lang, H.; Hietschold, M. *Surf. Sci.* **2014**, *628*, 92−97.
(60) Wang, Y.; Kröger, J.; Berndt, R.; Hofer, W. *Angew. Chem., Int. Ed.* **2009**, *48*, 1261−1265.

DOI: 10.1021/ja510528x
J. Am. Chem. Soc. 2015, 137, 1844−1849